PAPER Special Issue on 1992 International Symposium on Antennas and Propagation

A Consideration of the Thin Planar Antenna with Wire-Grid Model

Nozomu ISHII† and Kiyohiko ITOH†, Members

SUMMARY A theoretical and experimental study of a thin card-sized antenna is presented. The method of moment with a wire-grid model is used to analyze this antenna. In order to validate numerical efficiency, measurements using Wheeler method are preformed on this antenna and its wire-grid models. The experimental and theoretical results are in good agreement if the wire conductivity is well chosen. And the noise reduction of measured Wheeler efficiency using least mean square method is also examined.

key words: *card-sized antenna, wire-grid model, moment method, Wheeler method, radiation efficiency, least mean square method*

1. Introduction

Recently a small and thin antenna for the portable receiver is required as the personal wireless communication becomes more popular. However, such a antenna does not have good electrical characteristics. Especially, a card-sized antenna for the paging receiver has large mismatch loss and very small radiation efficiency because of the electrically small height of the antenna.

To analyze the electrical characteristics of this card-sized antenna and develop an advanced antenna which has better radiation and reflection efficiencies, it is desired to use a simple numerical method which leads accurate results and a technique to rapidly measure the radiation efficiency. In this paper, we replace plate parts of the antenna with corresponding wire-grid models [1] and apply the method of moment for the thin-wire structure proposed by Richmond [2] to these models. Although it is difficult to numerically analyze this type of antenna where electrically short wires attach to the perimeter of the plate, the accurate results can be obtained by this numerical method if we can approximate plate parts to suitable wire-grids and we can arrange expansion/test functions at proper positions.

However, the wire-gird model has a deficiency in setting the size of the grid and selecting the grid radius [3]. Physical backbone for the wire-grid modeling the quasi-electric approximation was reported [4], but accurate guideline for the grid approximation which is valid in the near field is still ambiguous. Sato et al. evaluated the performance of a monopole on rectangular body which modeled with wire-grid using the method of moment [5], and Morishita et al. analyzed a microstrip antenna which has a finite ground plane with wire-grid model [6]. Also, a card-sized antenna was analyzed by using the method of moment with wire-gird model [3]. In this paper, we will treat the radiation efficiency using numerical method with the wire-grid model and experimentally verify it by the Wheeler method.

The Wheeler method is known as an easy and rapid method to measure the radiation efficiency. In this method, it is only necessary to measure input resistances with and without a shielding cap which can cover the antenna under test [7],[8]. Its applications to a matched antenna based on two conductances [9],[10] or two reflection coefficients [11] were reported. Ida et al. applied this method to mismatched small loop antennas [12]. In this paper, we measure the radiation efficiency of the card-sized antenna which has very small radiation and reflection efficiencies and we compare measured results with numerical ones. Then we show that we can numerically estimate the radiation efficiencies if the wire conductivity is well chosen.

2. Overview of Analytical Method

We assume that an antenna is modeled with its wire-grid model. First, we divide the wire structure into V-shaped dipole elements [3], noting that $(n-1)$ independent V-shaped dipoles are set at the point with n branches. Then, we express the total current distribution $\overline{J}^s$ on this antenna in known expansion functions $\overline{J}_n$, corresponding the V-shaped dipoles with unit current density at the terminals;

$$\overline{J}^s = \sum_{n=1}^{N} I_n \overline{J}_n \tag{1}$$

where I_n is a sampling value of the function $\overline{J}_n$. From Eq.(1) and the zero reaction theorem [13], we obtain the following equations,

$$\sum_{n=1}^{N} Z_{mn} I_n = V_m \qquad \text{for} \quad m = 1, 2, \ldots, N, \tag{2}$$

where

$$Z_{mn} = -\iint_{S_n} \overline{J}_n \cdot \left[\overline{E}_m - (\hat{n} \times \overline{H}_m) Z_s\right] ds, \tag{3}$$

Manuscript received May 13, 1993.
Manuscript revised July 12, 1993.

†The authors are with Faculty of Engineering, Hokkaido University, Sapporo-shi, 060 Japan.

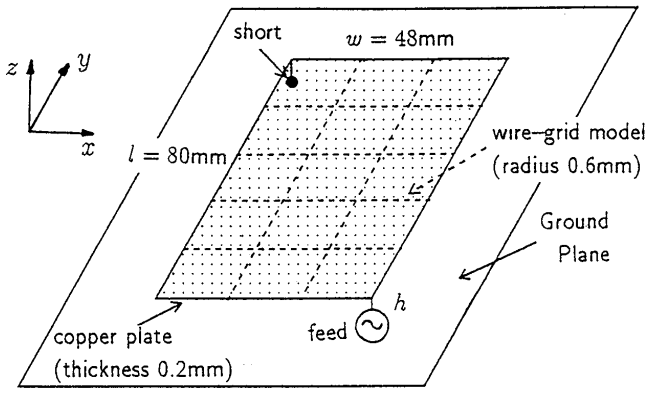

Fig. 1 A typical card-sized antenna for the paging.

$$V_m = \iint_{S_m} \overline{J}_m \cdot \overline{E}^i ds, \tag{4}$$

where Z_s denotes the surface impedance of the wire and the unit vector $\hat{n}$ is directed outward on the wire surface S_n. $(\overline{E}_m, \overline{H}_m)$ are the free-space fields of test-source $\#m$ and $\overline{E}^i$ is an impressed electric field. Z_{mn} is the mutual impedance between $\#m$ and $\#n$ dipoles and determined by the arrangement of two dipoles. V_m is the voltage at $\#m$ dipole and determined by feeding method.

In this paper, we use a piecewise sinusoidal function as expansion and test function. Arrangement of expansion and test dipoles is fixed throughout calculation of mutual impedances. For example, expansion dipoles are placed above the grid plane shifting with their radius [3] and test dipoles are expanded on the original plane in the case of an antenna shown in Fig. 1.

A detail discussion for the calculation of the mutual impedance between lossless two dipoles is given in [3]. In the case that the wire has a finite conductivity, we must take the surface impedance of the wire, Z_s, into account to evaluate an exact mutual impedance. In Eq.(3), an additional mutual impedance

$$\Delta Z_{mn} = Z_s \iint_{S_n \cap S_m} \overline{J}_n \cdot (\hat{n} \times \overline{H}_m) ds \tag{5}$$

is not zero if shared region between $\#m$ and $\#n$ dipoles exists. To evaluate ΔZ_{mn}, we require to calculate the additional mutual impedance between two monopoles which correspond to respective arms of two V-shaped dipoles, ΔZ_{ij} (refer to $\#i$ and $\#j$ in Fig. 2), since the mutual impedance between two dipoles is evaluated as the sum of four mutual impedances between monopoles [3]. After simple mathematical manipulations, we obtain

$$\Delta Z_{ij} = \begin{cases} \dfrac{Z_s}{2\pi a} \dfrac{2k\Delta z - \sin 2k\Delta z}{4k \sin^2 k\Delta z} & \text{(a)} \\ \dfrac{Z_s}{2\pi a} \dfrac{k\Delta \cos k\Delta z - \sin k\Delta z}{2k \sin^2 k\Delta z} & \text{(b)} \end{cases} \tag{6}$$

where $\#i$, $\#j$ monopoles are parallel for (a), anti-parallel for (b), as shown in Fig. 2, a denotes the wire radius, $k = \omega\sqrt{\mu\epsilon}$ and $\Delta z = z_1 - z_0$.

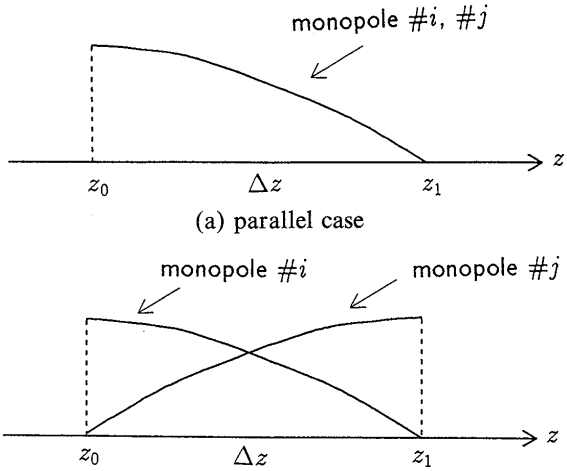

Fig. 2 A local coordinate system for calculating loss term of the additional mutual impedance between monopole $\#i$ and $\#j$.

To estimate the radiation efficiency, we need radiated power from the antenna. In general, the radiated electric field is given as

$$\overline{E} = -j\omega\mu \frac{e^{-jkr}}{4\pi r} (\hat{\theta} D_\theta + \hat{\phi} D_\phi) \tag{7}$$

where $\hat{\theta}$, $\hat{\phi}$ are the unit vectors in the θ, ϕ directions, D_θ, D_ϕ are the θ-, ϕ- components of the vector current moment defined as [13]

$$\overline{D} = \iiint \overline{J}(\overline{r}') e^{j\overline{k}\cdot\overline{r}'} dv' \tag{8}$$

The antenna current is expanded with N dipoles as Eq.(1), $\overline{D}$ can be expressed as follows:

$$(\hat{\theta} D_\theta + \hat{\phi} D_\phi) = \sum_{n=1}^{N} I_n (\hat{\theta} D_{\theta n} + \hat{\phi} D_{\phi n}) \tag{9}$$

where

$$D_{\theta n} = D^+_{\theta n} + D^-_{\theta n}$$
$$D_{\phi n} = D^+_{\phi n} + D^-_{\phi n}$$

$D_{\theta n}$, $D_{\phi n}$ are the θ, ϕ components of the vector current moment which is produced by the unit dipole $\#n$, and $D^\pm_{\theta n}$, $D^\pm_{\phi n}$ are corresponding to two monopoles of the dipole $\#n$. For example, an $\hat{s}$ directed monopole which has the surface current distribution

$$\overline{J}^+_n = \frac{\hat{s}}{2\pi a} \frac{\sin k(\Delta s - s)}{\sin k\Delta s}$$

as shown in Fig. 3, produces the following vector current moment

$$D^+_{\theta n} = (\hat{s} \cdot \hat{\theta}) J_0(ka\sqrt{1-\zeta^2}) e^{jk\hat{r}\cdot\overrightarrow{OP}} \cdot \frac{e^{jk\zeta\Delta s} - \cos k\Delta s - j\zeta \sin k\Delta s}{(1-\zeta^2) k \sin k\Delta s} \tag{10}$$

where $J_0(\cdot)$ is the Bessel function of order 0, $\hat{r}$ is the unit vector in the r direction, $\zeta = \hat{s} \cdot \hat{r}$ and $\Delta s = s_1 - s_0$. $D^+_{\phi n}$ is obtained by replacing θ with ϕ in Eq.(10).

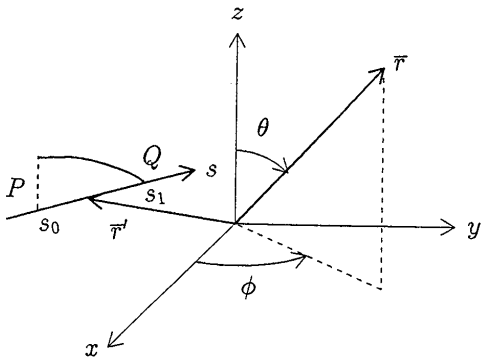

Fig. 3 A coordinate system for calculating the far-field of a monopole.

The total radiated power P_{rad} is given by

$$P_{rad} = \frac{k^2 Z}{(4\pi)^2} \int_0^{2\pi} d\phi \int_0^{\pi} (|D_\theta|^2 + |D_\phi|^2) \sin\theta d\theta \quad (11)$$

where $Z = \sqrt{\mu/\epsilon}$, and the total input power P_{in} given by

$$P_{in} = \sum_{n=1}^{N} V_n I_n^* \quad (12)$$

Since the radiation efficiency η is defined as the ratio of the radiated power given in Eq.(11) to the input power given in Eq.(12), it can be calculated using the following relation.

$$\eta = \frac{P_{rad}}{P_{in}} \quad (13)$$

3. Wheeler Method

The radiation can be removed little disturbing the near field, when the radiansphere of $\lambda/2\pi$ radius is replaced with corresponding shielding cap, because the stored energy and the power lost are mainly predominant in this sphere and the radiated power are related to the far-field outside the sphere [7]. Then, the input power of the antenna nearly equals the power lost, P_{loss}. By measuring P_{loss} and the input power without a shield, P_{in}, we obtain the radiation efficiency as follows:

$$\eta = 1 - \frac{P_{loss}}{P_{in}} \quad (14)$$

This technique for measuring the efficiency is known as the Wheeler method and this efficiency is referred as the Wheeler efficiency. If an antenna can be expressed by the series RLC circuit, Eq.(14) is reduced to [8]

$$\eta_r = 1 - \frac{R_{loss}}{R_{in}} \quad (15)$$

where R_{in} is the input resistance without the cap and R_{loss} is the loss resistance which can be measured as the input resistance with the cap. We should notice that this value is negative near the parallel-resonant frequency because of $R_{loss} > R_{in}$. Next, if the antenna can be modeled by the parallel RLC circuit, Eq.(14) is reduced to [9]

$$\eta_g = 1 - \frac{G_{loss}}{G_{in}} \quad (16)$$

where G_{in} and G_{loss} are the input conductances without and with the cap, respectively. In this case, η_g is negative near the series-resonant frequency because of $G_{loss} > G_{in}$. Thus, the estimation based on two resistances or two conductances is invalid in parallel or series resonant, respectively. When an equivalent circuit model for the antenna is complicated so that we can not use above series or parallel RLC circuit model, the Wheeler efficiency is given by [11]

$$\eta = 1 - \frac{1 - |\Gamma_{loss}|^2}{1 - |\Gamma_{in}|^2} = \frac{|\Gamma_{loss}|^2 - |\Gamma_{in}|^2}{1 - |\Gamma_{in}|^2} \quad (17)$$

where $|\Gamma_{in}|$ and $|\Gamma_{loss}|$ are the amplitudes of the reflection coefficients without and with the cap, respectively. Equation (17) is not based on loss mechanism of the antenna, but can be derived from Eq.(14) without approximation. Moreover, Eq.(15) or (16) is derived from Eq.(17) under series- or parallel-resonant condition (See Appendix). This is the reason why we adopt Eq.(17) as the Wheeler efficiency in the rest of this paper.

The Wheeler method was little applied to mismatched antennas with a large mismatch loss ($|\Gamma_{in}| \approx 1$) such as the card-sized antenna. Moreover, $|\Gamma_{loss}|$ with the cap is larger than $|\Gamma_{in}|$ without the cap. Therefore, the difference between $|\Gamma_{in}|$ and $|\Gamma_{loss}|$ is very small and out of the uncertainty range of measurement system (1.5% uncertainty at $|\Gamma| = 1$ below 2 GHz for a network analyzer HP8510B/C and a test set HP8515A which we used in our measurement) so that it is possible that the Wheeler efficiency would include errors due to the system uncertainty.

4. Numerical and Experimental Results

First, we consider a card-sized antenna composed of the rectangular copper sheet having $l = 80$ mm length and $w = 48$ mm width and two wires with height h as shown in Fig. 1. These sheet and wires are connected at two corners of sheet, one point is short-circuited on the ground and the other point is fed at the ground. A sample of the wire-grid model divided into 3 parts for the x direction and 5 parts for the y direction is also shown in Fig. 1.

Since the height of this antenna is much smaller than the dimension of the plate and the feeding point on the ground plane exists in close proximity to the wire gird, effects due to grid approximation are larger as the grid is coarser. Table 1 shows the relation between the parallel-resonant frequency and the grid division number for the wire-grid model which is divided into m

Table 1 Parallel-resonant frequency vs. division number of the grid.

	n=1	n=2	n=3
m=1	572 MHz	550 MHz	525 MHz
m=2	550 MHz	547 MHz	535 MHz
m=3	530 MHz	542 MHz	540 MHz
m=4	505 MHz	525 MHz	533 MHz
m=5	485 MHz	512 MHz	525 MHz

f_r : 532 MHz (Experiment)

parts for the y direction and n parts for the x direction. The wire radius of both grid and wire parts is 0.6 mm. In the case of n=1, the electric current in the y direction cannot express with the wire-gird model so that the parallel-resonant frequency is not converged to 532 MHz which is that of an original antenna model, as m is large number. For n=2, a similar tendency is observed. In the case of fixed m, the parallel-resonant frequency is smaller for $m \leqq 2$ and larger for $m \geqq 3$, as n is larger. When the geometry of the unit grid is close to square, the parallel-resonant frequency approaches to 532 MHz. We can also see that a proper grid approximation is required to express the electric current inside the plate as well as on the perimeter of the plate [5],[14].

Next, we examine the radiation efficiency of this antenna using both numerical method in Sect. 2 and Wheeler method in Sect. 3. The numerical efficiency is obtained by replacing the antenna with the wire-grid model and incorporating loss term given in Eq.(6) with the mutual impedance given in Eq.(3). In measuring the Wheeler efficiency, we should take care of

1. keeping constant temperature in the laboratory not to change calibration data until whole measurements are finished,
2. keeping the same cable curvature when calibration data and reflection coefficients of the antenna with/without a shielding cap are measured,
3. keeping electrical contact between the edge of the cap and the ground plane using steel wool or conductive tape,
4. placing the antenna under test in the center of the cap.

In addition to above remarks, we should start to measure after two hours' warming-up of the synthesized sweep oscillator (HP8340B). It was reported that the Wheeler efficiency is not critical for the conductivity and the shape of the shielding cap, but should be measured below the resonant frequency of the cap which forms an electric wall cavity with the ground plane. In this paper, we use a rectangular cap or a pseudo-hemisphere cap (mixing bowl) as the shielding cap, as shown in Fig. 4 and Table 2.

Figure 5 (a) shows the Wheeler efficiency of the antenna shown in Fig. 1 with $h=2$ mm versus frequency

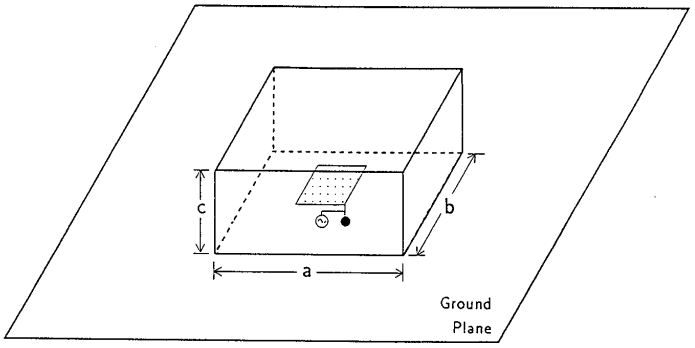

(a) rectangular cap

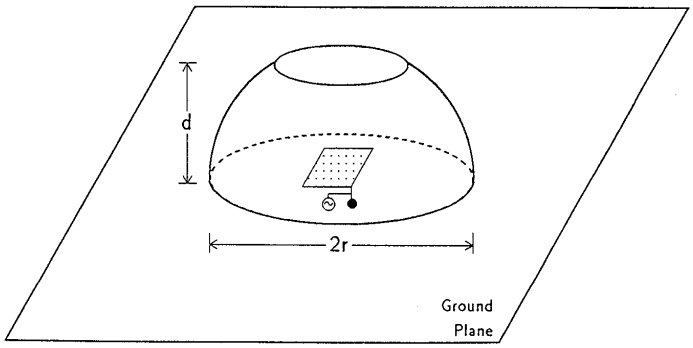

(b) pseudo-hemisphere cap

Fig. 4 Shape of the shielding cap.

Table 2 Types and dimensions of used shielding caps as shown in Fig. 4.

Rectangular Cap				Pseudo-Hemisphere Cap		
type	a[mm]	b[mm]	c[mm]	type	2r[mm]	d[mm]
A	140	140	75	C	210	80
B	160	160	75	D	240	90

using an aluminum rectangular cap (type-B). The measured curves in this figure are not smooth because of the uncertainty of the measurement system. Good agreement between copper sheet and wire-grid model is observed below 0.6 GHz so that we can estimate the Wheeler efficiency using the wire-grid model. Similar results are obtained by using any other cap which is listed in Table 2. For example, Fig. 5 (b) shows the result with a pseudo-hemisphere cap (mixing bowl, type-D). This fact makes us warrant that we can estimate the radiation efficiency by the method of moment with the wire-grid model if the wire conductivity is correctly chosen. Figures 5 (a), (b) show also two numerical efficiencies with the wire conductivity $\sigma_{Cu} = 5.8 \times 10^7$, 5.0×10^6 S/m. The numerical efficiency with $\sigma_{Cu} = 5.8 \times 10^7$ S/m is larger than the measured one because the conductivity of the wire which we used is smaller than the value given in the authorized table due to roughness of the wire surface and soldering loss. In practice, the numerical curve for $\sigma_{Cu} = 5.0 \times 10^6$ S/m is agreed with the measured one.

Figures 6 (a)–(d) show Wheeler efficiencies of this

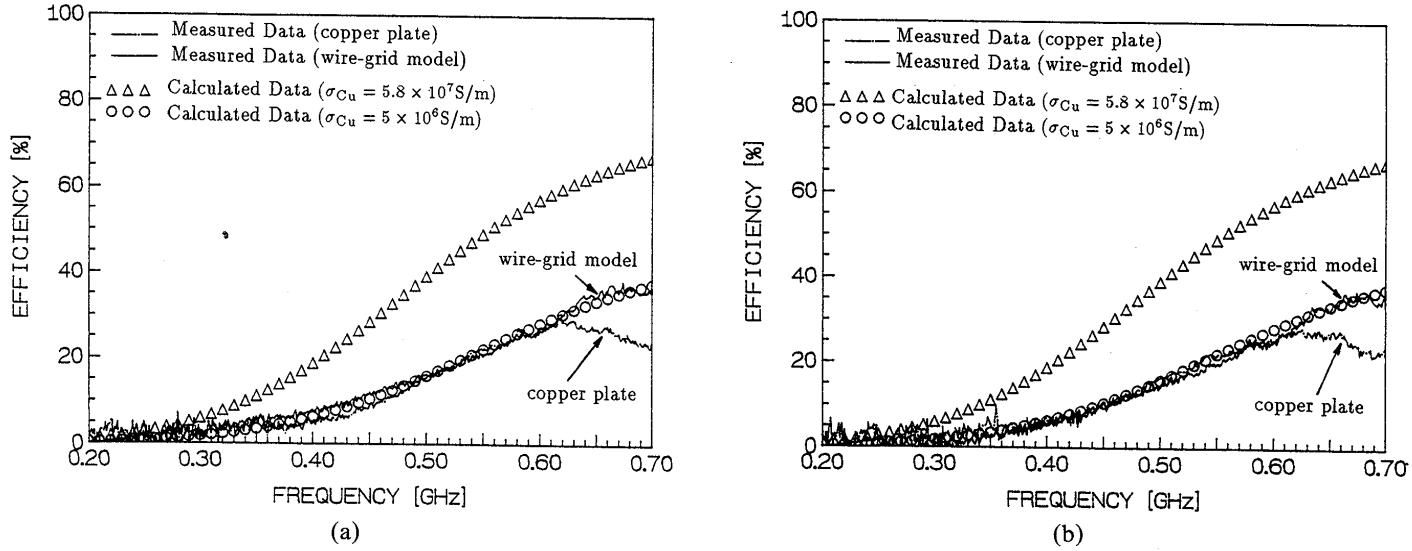

Fig. 5 Calculated and measured efficiency for the antenna shown in Fig. 1 [$h = 2$ mm], (a) with a type-B cap, (b) with a type-D cap.

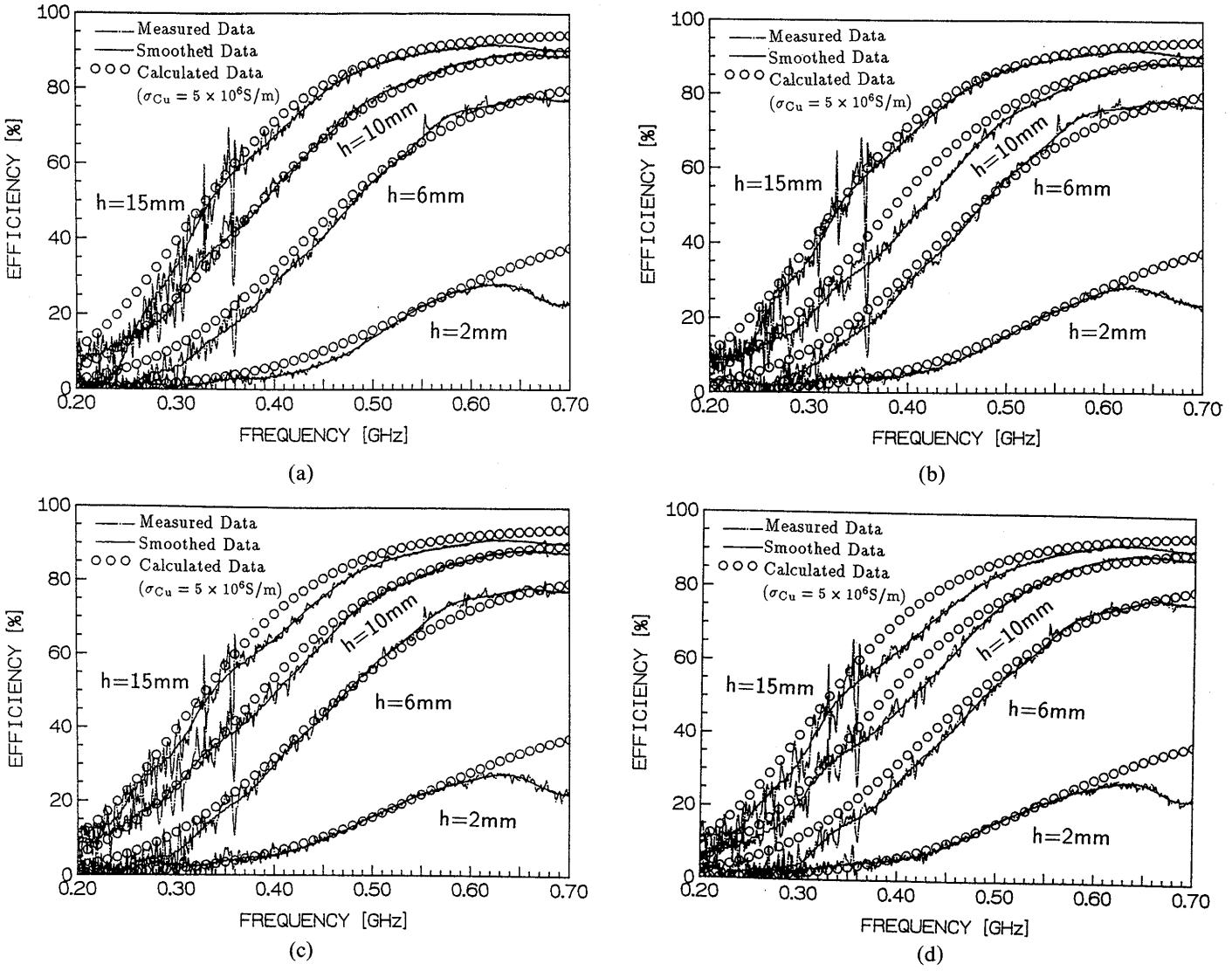

Fig. 6 Calculated, measured and smoothed efficiency for the antenna shown in Fig. 1 [h=2, 6, 10, 15 mm], (a) with a type-A cap, (b) with a type-B cap, (c) with a type-C cap, (d) with a type-D cap.

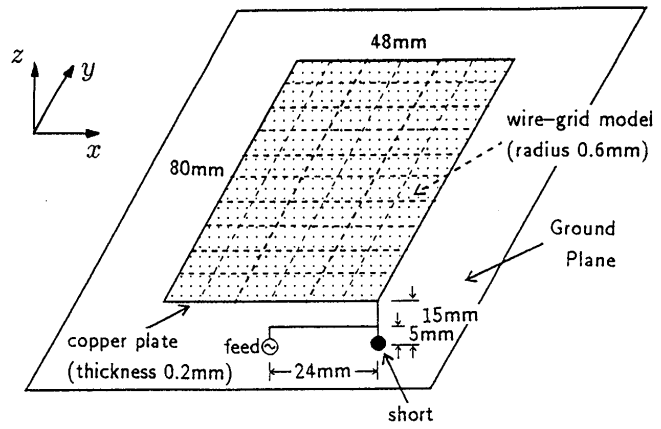

Fig. 7 A matched card-sized antenna

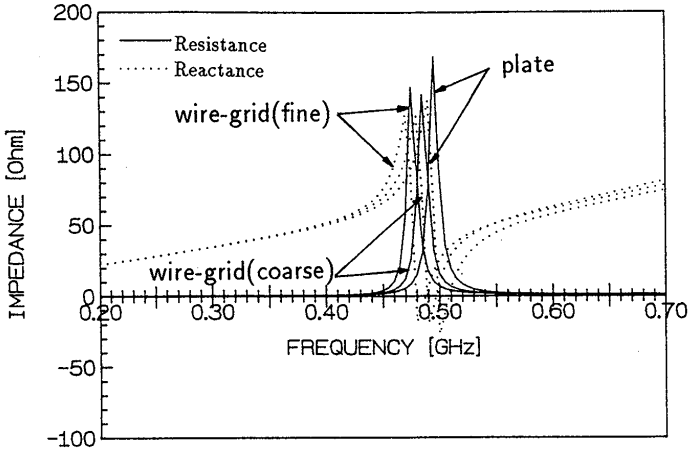

Fig. 8 Impedance vs. frequency for the antenna shown in Fig. 7.

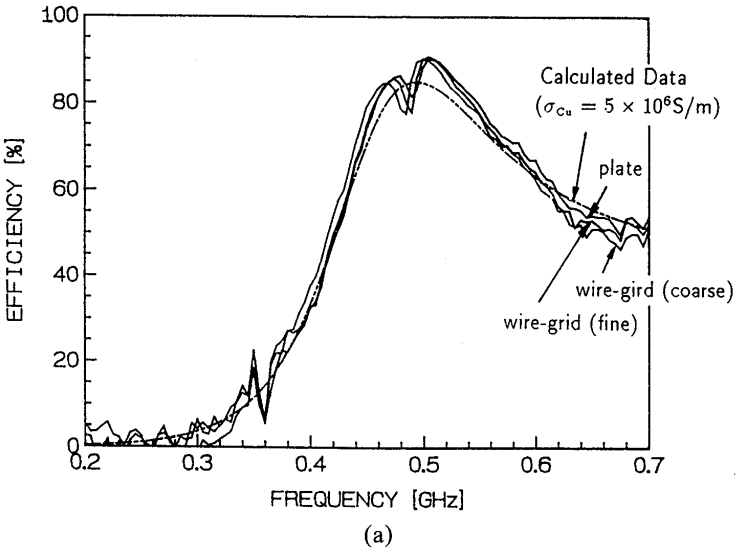

(a)

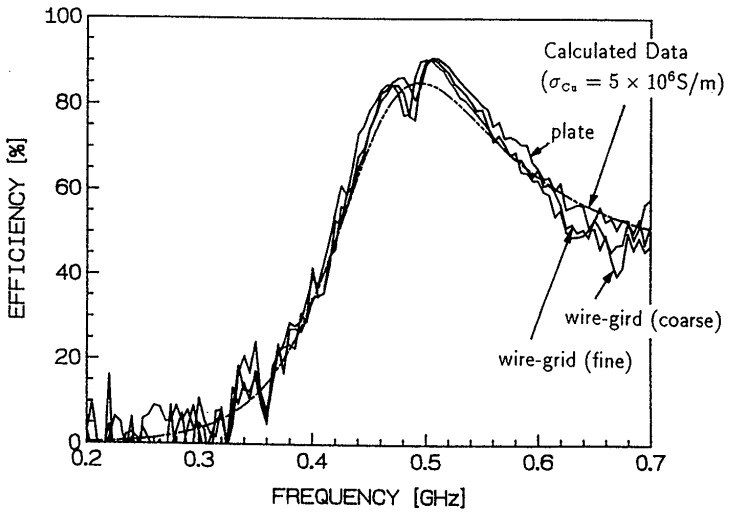

(b)

Fig. 9 Calculated and measured efficiency for the antenna shown in Fig. 7, (a) with a type-B cap, (b) with a type-D cap.

antenna with $h=2$, 6, 10, 15 mm using four caps as shown in Table 2. We can observe that the radiation efficiency is larger as the antenna height h is larger and the frequency is higher. In these figure, calculated data using 3×5 wire-grid model with the conductivity $\sigma_{Cu}=5.0\times10^6$ S/m and the gird radius $a_g=0.6$ mm are also plotted. These numerical results are agreed with experimental ones for each h and cap, so that this fact ensures the validity of our numerical efficiency estimation and we suppose that the conductivity of the wire and the copper sheet which is used in our experiment is 5.0×10^6 S/m. This supposition may be dependent on

1. the resistance due to soldering [12],
2. the precision in handiwork of the antenna, especially its height, h,
3. the time-variation of the calibration data (We calibrate the system every 20–30 minutes.),

but we assume $\sigma_{Cu} = 5.0\times10^6$ S/m (constant) throughout this paper. And from Figs. 6 (a)–(d), we also see that the Wheeler efficiency is not affected by the shape and the dimension of the cap.

The card-sized antenna shown in Fig. 1 is not matched to the feeding line so that the Wheeler method is suitable for measuring its efficiency, because this method is not required to insert a matching section (for example, L-section network with two capacitors [3]) or modify the feeding part of the antenna for matching. In general, matching is not achieved over wide band-width so that it is difficult to measure the efficiency using any other method which is required self-matching of the antenna. However, the Wheeler method is available as long as the antenna can be covered by a conducting cap.

Now, we consider a self-matched card-sized antenna based on the principal of Γ-junction [15]. As shown in Fig. 7, this antenna has the same plate part of the antenna as shown in Fig. 1, but the feeding part is more complicated. Figure 8 shows measured input impedances of this antenna, 3×5(coarse) and 6×10(fine) wire-grid models as shown in Fig. 7. These results agree with each other so that we can approximate this antenna to these wire-grid model. Figure 9 (a) shows the Wheeler efficiencies of this antenna and two wire-

grid models using a rectangular cap (type-B) and the calculated efficiency using 3×5 wire-grid model with $\sigma_{Cu} = 5.0 \times 10^6$ S/m. Measured results using a mixing bowl made of stainless steel (type-D) as a shielding cap are shown in Fig. 9 (b). From these figures, calculated efficiency is agreed with experimental data without regard for the shape of the shielding cap. Measured curves for the bowl cap have more spurious noise than the rectangular cap because the electrical contact between ground plane and edge of the cap would be worse than the rectangular cap. Around the matching frequency (495 MHz), a dimple of the Wheeler efficiency is observed. In the Wheeler method, we assume that the reactive energy is not changed by the existence of the shielding cap. However, in the case of the well-matched antenna, the variation of the reactive energy which corresponds on the input impedance or admittance is large near series- or parallel-resonant frequency. Moreover, the series- or parallel-resonant frequency with a cap is not the same without a cap [16]. Therefore, the dimple of the Wheeler efficiency is remarkably observed near the resonant frequency.

By the way, the noise on the measured curve can be reduced by narrowing the IF bandwidth [12], but in our system (HP8510B/C) the IF bandwidth is fixed at 10kHz so that we can not narrow this bandwidth. So, we consider the noise reduction with the least mean square polynomial fitting technique (LMSPF) which is useful to reduce the Gaussian noise on the measured curve. This noise is caused by the uncertainty of the measured reflection coefficient and is generally random for the frequency. Therefore, the noise would be reduced by smoothing two amplitudes of the reflection coefficients $|\Gamma_{in}|$ and $|\Gamma_{loss}|$ by the LMSPF as function of the frequency, f. That is, we approximate measured data $|\Gamma|^2$ to a polynomial function

$$|\Gamma|^2 = a_0 + a_1 f + a_2 f^2 + \cdots + a_n f^n,$$

where a_i, $i = 1, 2, \cdots, n$ are constants determined by the LMSPF algorithm, and n is order of the polynomial which is determined to trace two measured $|\Gamma|^2$ curve smoothly. Figures 6 (a)–(d) also show the smoothed results of n =21 for the Wheeler efficiency of the antenna shown in Fig. 1, which are generated from 461 point data (170 MHz–730 MHz). As seen from these figures, we can see that this smoothing technique is effective for the noise reduction of the measured efficiency, that is, we can pick up the Wheeler efficiency with a reasonable accuracy from noisy data by using the LMSPF.

5. Conclusion

This paper has presented a numerical analysis for the radiation efficiency of a card-sized antenna using the method of moment and the wire-grid model with results which agreed well measured data by the Wheeler method if the wire conductivity is properly given. In this work, the Wheeler efficiency was estimated by two measured reflection coefficients. This estimation do not fail at parallel- or series-resonant frequency where estimation using two resistances or two conductances leads negative efficiency respectively. However there is one drawback to the Wheeler method in that the dimple of the efficiency appears near the resonant frequency where matching is well achieved. And the noise reduction technique using the least mean square curve fitting is useful for the accurate estimation of the Wheeler efficiency.

Acknowledgment

This work was supported by Grant-in-Aid for Scientific Research 62420033 from the ministry of Education, Science and Culture of Japan.

References

[1] Richmond, J.H., "Wire-Grid Model for Scattering by Conducting Bodies," *IEEE Trans. Antennas Propag.*, vol.AP-14, no.6, pp.782–786, Nov. 1966.
[2] Richmond, J.H. and Geary, N.H., "Mutual Impedance of Nonplanar-Skew Sinusoidal Dipoles," *IEEE Trans. Antennas Propag.*, vol.AP-23, no.3, pp.412–414, May 1975.
[3] Ishii, N. and Itoh, K., "Analysis on Small Planar Antenna in a Paging System," *IEICE Trans.*, vol.E74, no.10, pp.3233–3240, Oct. 1991.
[4] Lee, K.S.H., Martin, L. and Castillo, J.P., "Limitations of wire-grid modeling of a closed surface," *IEEE Trans. Electomag. Compat.*, vol.EMC-18, no.3, pp.123–129, Aug. 1976.
[5] Sato, K., Matsumoto, K., Fujimoto, K. and Hirasawa, K., "Characteristics of a Planar Inverted-F Antenna on a Rectangular Conducting Body," *Trans. IEICE*, vol.J71-B, no.11, pp.1237–1243, Nov. 1988.
[6] Morishita, H., Fujimoto, K. and Hirasawa, K., "Analysis of Rectangular Microstrip Antenna Having the Same Width as the Ground Plane," *Trans. IEICE*, vol.J71-B, no.11, pp.1274–1280, Nov. 1988.
[7] Wheeler, H.A., "The Radiansphere Around a Small Antenna," *Proc. IRE*, vol.47, no.8, pp.1325–1331, Aug. 1959.
[8] Newman, E.H., Bohley, P. and Walter, C.H., "Two Methods for the Measurement of Antenna Efficiency," *IEEE Trans. Antennas Propag.*, vol.AP-23, no.4, pp.457–461, Jul. 1975.
[9] Ando, M., Ishida, S. and Itoh, K., "Efficiency Measurement of Electrically Small Antenna Using Wheeler Cap Method," *1987 Spring National Convention Record, IECE*, vol.3, S8-1.
[10] Pozar, D.M. and Kaufman, B., "Comparison of Three Methods for the Measurement of Printed Antenna Efficiency," *IEEE Trans. Antennas Propag.*, vol.36, no.1, pp.136–139, Jan. 1988.
[11] Sakurai, K., Kikuchi, H., Arai, H., Ando, M. and Goto, N., "Measurements of Antenna Efficiency Using Scaled Models by Wheeler Method," *1987 Spring National Convention Record, IEICE*, vol.3, S8-3.
[12] Ida, I., Fujisawa, T., Ito, K. and Takada, J., "A Study on Measurement of Radiation Efficiency of Small Loop Antennas," *IEICE Technical Report*, A·P92-63, RCS92-51, Jul. 1992.

[13] Kong, J.A., *Electromagnetic Wave Theory* (2nd edition), John Wiley & Sons, New York, 1990.
[14] Lin, Y.T. and Richmond, J.H., "EM Modeling of Aircraft at Low Frequencies," *IEEE Trans. Antenna Propag.*, vol.AP-23, no.1, pp.53–56, Jan. 1975.
[15] Stutzman, W.L. and Thiele, G.A., *Antenna Theory and Design*, John Wiley & Sons, New York, 1981.
[16] Chao, R., Hirasawa, K. and Fujimoto, K., "On the Wheeler Cap Method," *IEICE Technical Report*, A·P88-47, Aug. 1988.

Appendix A: Derivation of η_r, η_g from η

If z_{in} is normalized input impedance without the shielding cap and z_{loss} is with the cap, Eq.(17) reduces to

$$\eta = 1 - \left|\frac{1+z_{in}}{1+z_{loss}}\right|^2 \frac{r_{loss}}{r_{in}} \qquad (A\cdot 1)$$

where $r_{loss} = \mathrm{Re}(z_{loss})$ and $r_{in} = \mathrm{Re}(z_{in})$. At the frequency in the series-resonant, $\mathrm{Im}(z_{loss}) = \mathrm{Im}(z_{in}) = 0$, $r_{loss} \ll 1$ and $r_{in} \ll 1$, then,

$$\eta \approx 1 - \frac{r_{loss}}{r_{in}} = 1 - \frac{R_{loss}}{R_{in}} = \eta_r \qquad (A\cdot 2)$$

On the other hand, at the frequency in the parallel-resonant, $\mathrm{Im}(z_{loss}) = \mathrm{Im}(z_{in}) = 0$, $r_{loss} \gg 1$ and $r_{in} \gg 1$, then,

$$\eta \approx 1 - \frac{r_{in}}{r_{loss}} = 1 - \frac{G_{loss}}{G_{in}} = \eta_g \qquad (A\cdot 3)$$

These two expressions (A·2) and (A·3) fail to estimate the Wheeler efficiency in the opposite resonant, since η_s and η_g are derived under the series- and parallel-resonant conditions, respectively.

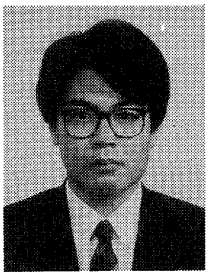

Nozomu Ishii was born in Sapporo, Japan, on October 8, 1966. He received the B.S. and M.S. degrees from Hokkaido University, Sapporo, Japan, in 1989, 1991, respectively. In 1991, he joined the faculty of Engineering at Hokkaido University, where he is currently a Research Associate of Electronic Engineering. His current research interests are in the area of numerical analysis of small antenna. He is a member of the IEEE.

Kiyohiko Itoh was born in Sapporo, Japan, on May 15, 1939. He received the B.S.E.E., M.S., and Ph.D. degrees from Hokkaido University, Sapporo, Japan, in 1963, 1965, and 1973, respectively. Since 1965, he has been on the faculty of Engineering at Hokkaido University, where he is currently a Professor of Electronic Engineering. During 1970–1971, he was with the Department of Electrical and Computer Engineering, Syracuse University, Syracuse, NY, as a Research Associate, on leave from Hokkaido University. His special interests are in electromagnetic radiation, wave optics, mobile communications, and solar power satellites. He is a member of the IEEE and the Institute of Television Engineering of Japan.